

REPORT DOCUMENTATION PAGE					Form Approved OMB No. 0704-0188	
<p>The public reporting burden for this collection of information is estimated to average 1 hour per response, including the time for reviewing instructions, searching existing data sources, gathering and maintaining the data needed, and completing and reviewing the collection of information. Send comments regarding this burden estimate or any other aspect of this collection of information, including suggestions for reducing the burden, to the Department of Defense, Executive Services and Communications Directorate (0704-0188). Respondents should be aware that notwithstanding any other provision of law, no person shall be subject to any penalty for failing to comply with a collection of information if it does not display a currently valid OMB control number.</p> <p>PLEASE DO NOT RETURN YOUR FORM TO THE ABOVE ORGANIZATION.</p>						
1. REPORT DATE (DD-MM-YYYY) 13-02-2012		2. REPORT TYPE Conference Proceedings			3. DATES COVERED (From - To)	
4. TITLE AND SUBTITLE Estimating Uncertainties in Bio-Optical Products Derived from Satellite Ocean Color Imagery Using an Ensemble Approach				5a. CONTRACT NUMBER		
				5b. GRANT NUMBER		
				5c. PROGRAM ELEMENT NUMBER 0602435N		
6. AUTHOR(S) Richard Gould, Sean McCarthy, Igor Shulman, Emanuel Coelho, James Richman				5d. PROJECT NUMBER		
				5e. TASK NUMBER		
				5f. WORK UNIT NUMBER 73-6467-01-5		
7. PERFORMING ORGANIZATION NAME(S) AND ADDRESS(ES) Naval Research Laboratory Oceanography Division Stennis Space Center, MS 39529-5004					8. PERFORMING ORGANIZATION REPORT NUMBER NRL/PP/7330-11-0814	
9. SPONSORING/MONITORING AGENCY NAME(S) AND ADDRESS(ES) Office of Naval Research One Liberty Center 875 North Randolph Street, Suite 1425 Arlington, VA 22203-1995					10. SPONSOR/MONITOR'S ACRONYM(S) ONR	
					11. SPONSOR/MONITOR'S REPORT NUMBER(S)	
12. DISTRIBUTION/AVAILABILITY STATEMENT Approved for public release, distribution is unlimited.						
<div style="font-size: 2em; font-family: cursive;">20120217364</div>						
13. SUPPLEMENTARY NOTES						
14. ABSTRACT <p>We propose a methodology to quantify errors and produce uncertainty maps for satellite-derived ocean color bio-optical products using ensemble simulations. Ensemble techniques have been used by the environmental numerical modeling community to propagate initialization, forcing, and algorithm error sources through-out the full simulation process, but similar approaches have not yet been applied to satellite optical properties. Uncertainties in retrievals of bio-optical properties from satellite ocean color imagery are related to a variety of factors, including sensor calibration, atmospheric correction, and the bio-optical inversion algorithms. Errors propagate, amplify, and intertwine along the processing path, so it is important to understand how the errors cascade through each step of the analysis, to assess their impact and identify the main factors contributing to the uncertainties in the final products. Also, we are interested in producing short-term forecasts of the bio-optical property distributions, by coupling the satellite imagery with physical circulation models. So, in addition to the uncertainties in the satellite-derived bio-optical properties due to the above-mentioned factors, the uncertainties in the model currents used to advect the bio-optical properties add another layer of complexity to the problem. We outline these processes and present preliminary results for this approach.</p>						
15. SUBJECT TERMS remote sensing, bio-optics, ocean color, error analysis, uncertainties, ensembles, forecasting						
16. SECURITY CLASSIFICATION OF:			17. LIMITATION OF ABSTRACT UU	18. NUMBER OF PAGES 16	19a. NAME OF RESPONSIBLE PERSON Richard Gould	
a. REPORT Unclassified	b. ABSTRACT Unclassified	c. THIS PAGE Unclassified			19b. TELEPHONE NUMBER (Include area code) 228-688-5587	

Estimating uncertainties in bio-optical products derived from satellite ocean color imagery using an ensemble approach

Richard W. Gould, Jr.*^a, Sean C. McCarthy^a, Igor Shulman^a, Emanuel Coelho^b, James Richman^c

^aNaval Research Laboratory, Code 7331, Stennis Space Center, MS, USA 39529;

^bUniversity of Southern Mississippi, Stennis Space Center, MS, USA 39529;

^cNaval Research Laboratory, Code 7323, Stennis Space Center, MS, USA 39529

ABSTRACT

We propose a methodology to quantify errors and produce uncertainty maps for satellite-derived ocean color bio-optical products using ensemble simulations. Ensemble techniques have been used by the environmental numerical modeling community to propagate initialization, forcing, and algorithm error sources through-out the full simulation process, but similar approaches have not yet been applied to satellite optical properties. Uncertainties in retrievals of bio-optical properties from satellite ocean color imagery are related to a variety of factors, including sensor calibration, atmospheric correction, and the bio-optical inversion algorithms. Errors propagate, amplify, and intertwine along the processing path, so it is important to understand how the errors cascade through each step of the analysis, to assess their impact and identify the main factors contributing to the uncertainties in the final products. Also, we are interested in producing short-term forecasts of the bio-optical property distributions, by coupling the satellite imagery with physical circulation models. So, in addition to the uncertainties in the satellite-derived bio-optical properties due to the above-mentioned factors, the uncertainties in the model currents used to advect the bio-optical properties add another layer of complexity to the problem. We outline these processes and present preliminary results for this approach.

Keywords: remote sensing, bio-optics, ocean color, error analysis, uncertainties, ensembles, forecasting

1. INTRODUCTION

Monte-Carlo methods have been applied in meteorology and physical oceanography to predict model errors and to improve weather and oceanic forecasts¹, by perturbing the dominant sources of uncertainties (e.g. initial conditions, model physics, etc), but similar approaches have yet to be applied to satellite optical properties and forecasts. Typically, to address uncertainties in water reflectances and bio-optical properties, satellite retrievals are compared to in situ measurements², but this approach has limitations. There are many errors and sources of uncertainty associated with operational forecasting, regardless of the forecast property. These include incomplete and/or inaccurate observations, uncertainties introduced through data assimilation, and unresolved dynamics and instabilities. The Monte-Carlo ensemble techniques (multi-analysis with a single model or algorithm) are then based on repeated model realizations with different initial and boundary conditions, atmospheric forcing, resolution, included data sets, bathymetry grids, and coefficient values, for example. An ensemble reflects therefore known sources of forecast uncertainty, and allows them to be evaluated³. There are several way to generate the parameter perturbations for the ensembles, including random bootstrapping from normal distributions for surface drift problems⁴, or subspace methods such as the Ensemble Transform for initial field estimations. Similar approaches can be applied to physical or optical properties.

Super-ensemble techniques (multi-model forecasts or algorithms) generalize the standard approach by enabling comparison of different models⁵⁻⁷. As a result, each ensemble realization will no longer be equally likely and bias corrections can be obtained by looking to the model skills at different scales. Using super-ensembles, we can “blend” multiple algorithms to optimize results. Statistics and metrics have been utilized (ensemble mean, RMS error, and spread) to provide some estimate of how well the ensembles capture “reality,” thereby providing insight into the underlying deterministic processes and aiding decision support. Statistical bias of the models can be determined from multiple linear regressions of the forecasts against observational fields. This methodology has been successfully applied in the ocean for surface drift problems and sound speed profile estimation; it can also be used to perturb the physics or internal model parameters and allows fast tuning (or calibration) of mesoscale ocean nests to specific areas and data sets.

*Richard.Gould@nrlssc.navy.mil; phone 1 228 688-5587; fax 1 228 688-4149; <http://www7331.nrlssc.navy.mil/>

Model and algorithm parameters can also be adjusted using ensemble techniques, to optimize performance and forecast skill. Also, of particular interest to the Navy, ensemble forecasts have been used to provide probabilistic forecasts, which in many cases could be more valuable than best guess forecasts to the warfighter for mission and contingency planning.

There are currently many new, advanced algorithms in the field of ocean color remote sensing (atmospheric correction, bio-optical inversion, vertical profile models, advection schemes for optical forecasts, electro-optical sensor performance models) for which the errors and uncertainties have not been adequately evaluated and characterized. The errors propagate through each step in the processing, from initial calibration of the satellite radiance data through the final estimates of target detection/identification. Estimation of uncertainty in ocean color satellite imagery is needed for most data assimilation schemes. Melding of observations and model predictions via data assimilation schemes is based on their prior uncertainty estimates. Therefore, observational and model forecast error covariances are fundamental components of most existing data assimilation approaches (including Kalman filters and smoothers, variational and hybrid approaches, etc). Although ensemble-based methodologies have been applied by the modeling community to help constrain model initial fields and boundary conditions, and to gain a better understanding of uncertainties associated with model results, these techniques have not been applied to ocean color satellite imagery.

Therefore, a strong requirement exists to provide the users of the optical properties, including bio-optical physical modelers who will assimilate the imagery and Navy mission planners and warfighters, with estimates of uncertainty in the derived satellite optical products. New measurement systems are now available with optical instrumentation (gliders, scanfish, moorings) and new satellite sensors are coming online (HICO, VIIRS) to help constrain the data ranges and calibrate the ensembles, so the time is right to develop these methodologies for ocean color. Application of ensemble techniques to satellite ocean color processing will greatly improve the value of the derived optical products to the end-users.

Our objective is to develop and evaluate methodologies to employ ensemble techniques to satellite ocean color data, to ultimately improve atmospheric correction and bio-optical inversion algorithms. By performing quantitative error evaluations and error cascading to estimate uncertainties in satellite-derived surface bio-optical properties, this approach will provide important new information in the form of error maps and will optimize the accuracy and value of the optical properties, rather than providing only "best guess" optical products to end-users as has been done in the past. We will gain a better understanding of the uncertainties at all levels of the processing of satellite ocean color imagery. In addition, the uncertainty estimates will accompany optical fields assimilated into coupled biophysical ecological models, improving downstream model forecast results.

2. METHODS

We are developing, evaluating, and applying ensemble methodology to satellite ocean color imagery. We will extend advances by the numerical modeling community to represent observational and algorithm error sources for ocean ensembles, and we will evaluate the ensemble representations and assess ensemble metrics. The ensemble approach will be applied at several levels: on the initial satellite data (radiances), on the atmospheric correction scheme, on the bio-optical inversion algorithms used to derive the optical properties (partitioned absorption coefficients, backscattering coefficients, chlorophyll concentration, suspended particulates, diffuse attenuation, and euphotic depth), on the second-order optical products derived for Navy applications (diver visibility, laser penetration, probability of target detection/identification), and finally on the optical field forecast distributions derived from coupling image products with circulation models. This will enable us to examine the effects of error propagation on the end-to-end processing. Here, we focus on uncertainties due to just two of these aspects, the first and last items above. First, we examine the effect of introducing noise to the top-of-atmosphere (TOA) satellite radiance values, and second, the effect of perturbations to the initial forcing of the physical circulation model used to advect the bio-optical properties (chlorophyll, in this case). A companion paper presented at this conference⁸ addresses aspects of uncertainties related to the atmospheric correction; future work will address the remaining components. The steps are illustrated schematically in Figure 1 and involve adapting methodology from numerical modeling to bio-optical remote sensing.

Several steps are required to accomplish these goals. We must first calculate expected ranges of variability in satellite measurements of the spectral remote sensing reflectances at regional scales from an image archive. Also, existing data sets collected during field campaigns will be mined and assessed for suitability as training data sets. The selected data sets should contain as complete a set of optical measurements as possible, covering all parameters estimated with the satellite inversion algorithms. The data sets should also cover a wide range of optical conditions, from turbid, optically-

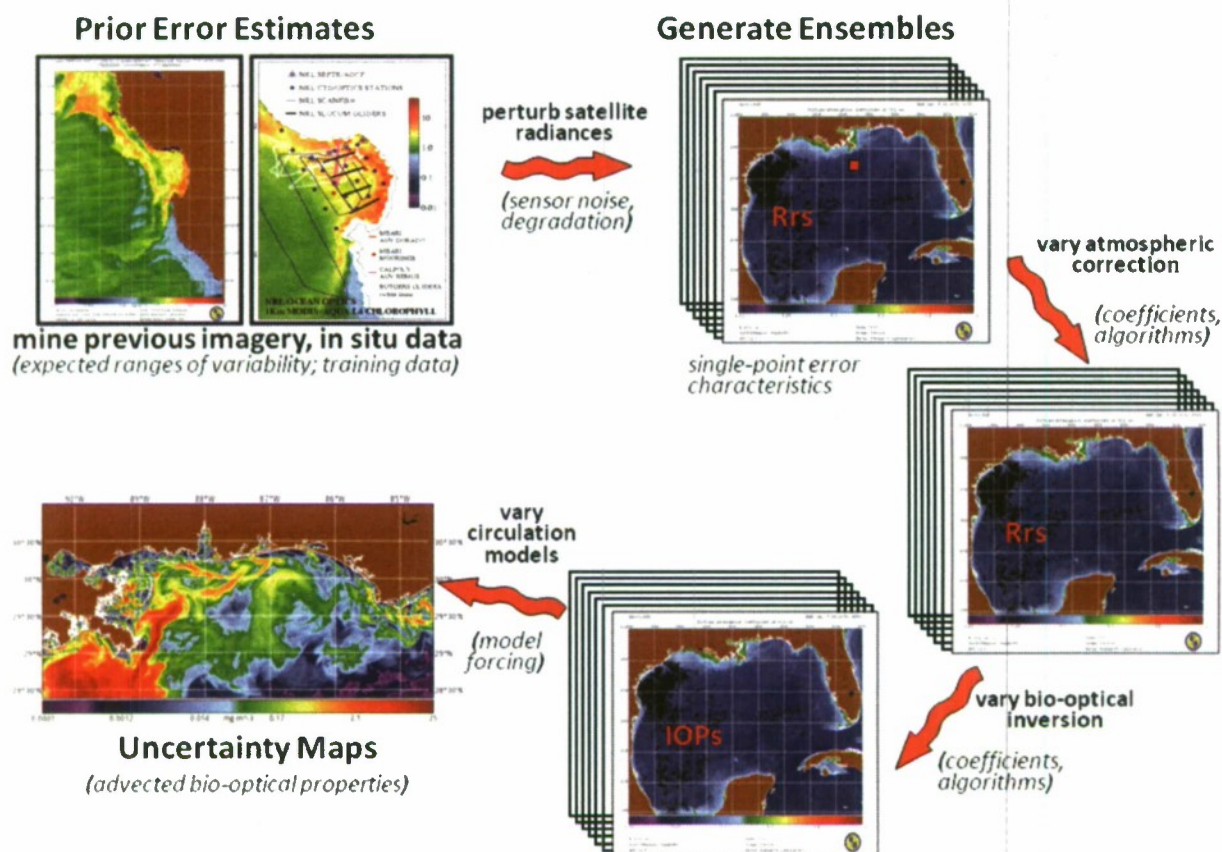


Figure 1. Schematic illustrating the steps involved with estimating bio-optical property uncertainties using an ensemble approach. Uncertainties at each stage of the processing contribute to the final, cumulative error map.

complex coastal waters, to clear, open-ocean waters. Our analyses using a wide variety and range of in situ and satellite optical data from open-ocean and coastal areas covering varied environmental conditions will enable us to form realistic ensembles that mimic real environmental variability and appropriately constrain and calibrate the ensembles. This will lead to accurate estimates of product uncertainties, which are required for assimilation of the bio-optical products into models. Initially, we will develop ensembles at a single point to determine error propagation characteristics. Then, we will extend the approach to an entire satellite image to assess spatial error characteristics, and to a sequence of imagery to examine temporal error characteristics.

The satellite imagery was processed using the NRL Automated Processing System (APS), which is capable of processing real-time and archived AVHRR, SeaWiFS, MODIS, and MERIS satellite imagery. APS is a powerful, extendable, image-processing tool; it is a complete end-to-end system that includes sensor calibration, atmospheric correction (with near-infrared correction for coastal waters), and bio-optical inversion. APS incorporates, and is consistent with, the latest NASA MODIS code (SeaDAS) and enables us to produce the NASA standard SeaWiFS and MODIS products, as well as Navy-specific products using NRL algorithms⁹. The automated, batch processing capability of APS allows us to rapidly process a suite of single point or image ensembles (based on adjusted radiance values and/or algorithm coefficients) to facilitate calculation of product errors.

To advect the surface SeaWiFS satellite chlorophyll field and produce 24, 48, and 72-hour forecast simulations, we used currents derived from the Relocatable Navy Coastal Ocean Model (RELO-NCOM). RELO-NCOM is based on a standardized development and an efficient configuration management to facilitate transitions of new tools and real-time configurations of regional high resolution (order 1 km) ocean predictions. The physics and numerical procedures of NCOM are based on the Princeton Ocean Model (POM) and a Sigma/Z-level Model (SZM). It solves a three-

dimensional, primitive equation, baroclinic, hydrostatic and free surface system using a cartesian horizontal grid, a combination of σ/z level (i.e., bottom-following/constant depth) vertical grid and implicit treatment of the free surface¹⁰. For mesoscale real-time applications, boundary conditions are taken from an operational run of the global NCOM (GNCOM). The domain of this particular experiment covered the entire Gulf of Mexico (18N 98W, 40N 79W), from 1 April to 30 October 2010. The atmospheric forcing was taken from the regional 15km COAMPS run by the Fleet Numerical Meteorological and Oceanographic Center (FNMOC). Tides were introduced at the boundaries and through local tidal potentials. The horizontal grid spacing was set at 3km and used 50 sigma/z levels in the vertical. The model assimilates local in-situ observations along with satellite altimetry and sea-surface temperature (SST) data using a combination of model analysis and data; all available observations from global and local data bases were assimilated over the full period.

For the chlorophyll forecasts, a “pseudo 3-dimensional” Eulerian advection scheme was used (without molecular or turbulent diffusion terms). With this approach, there are essentially two vertical layers, a 1 meter-thick surface layer and a conceptual deep layer to preserve continuity (i.e., there is vertical flux between the two layers, but they move together horizontally). These simulations only include current advection and an assumed uniform vertical chlorophyll distribution based on the surface values. Future enhancements will include addition of diffusion terms, full 3D vertical layering, and the capability to include more realistic vertical chlorophyll profiles. The forecast simulations do not include any assimilation of in situ chlorophyll data or additional satellite imagery, so currently the values are unconstrained. Also, with this approach, there is an implicit assumption that the bio-optical property (chlorophyll) is conservative. Although this is not strictly true, of course, it may be approximately valid over the short time scales (1-3 days) that we are examining, particularly in coastal areas where transport processes might be expected to dominate biological processes. Therefore, we consider the optical properties to be “pseudo-conservative” tracers for our purposes. This allows us to ignore growth and grazing terms and treat the distributional changes as though they are due entirely to dynamical processes¹¹.

3. RESULTS

3.1 Top-of-atmosphere radiance sensitivity test

We conducted sensitivity tests by applying noise (measurement uncertainty) to the TOA satellite radiance values. The goal is to add noise (random, or directional to simulate sensor drift or degradation over time) and propagate this noise through each step along the processing path, to assess the effect on uncertainties in the estimated inherent optical property (IOP) retrievals. First, we examine the effect of adding noise to the TOA total radiance in the 748 nm band ($L_t(748)$) on the calculated epsilon value ($\epsilon = L_t(748)/L_t(869)$ for MODIS). Epsilon is used to select the ocean color atmospheric correction models used to estimate the spectral aerosol radiance. Thus, errors in ϵ will lead to errors in aerosol radiance at 412 nm ($L_a(412)$), and subsequently to errors in the estimates of normalized water-leaving radiance at 412 nm ($nL_w(412)$) and bio-optical properties. Specifically, we will assess resulting errors in the absorption coefficient at 412 nm, $a(412)$, the backscattering coefficient at 547 nm, $b_b(547)$, and the chlorophyll concentration, chl. In addition, these tests allow us to assess how much change in $L_t(748)$ is required to change the selection of the aerosol models.

We generated the test set of TOA radiance ensembles by drawing 50 samples from a specified noise distribution described below. The final results show the variability (% difference) in the derived bio-optical properties due to the addition of noise. We have applied this approach at a single pixel; work is underway to generate and apply ensembles at each image pixel across an entire ocean color image to obtain uncertainty maps for the bio-optical products. At this point, we are only considering uncertainty due to the addition of TOA noise, and no other error sources.

First, we picked a random day, 19 March 2009, near Venice, Italy, to use for our single-point evaluation. The selected image pixel corresponds to the location of an Aerosol Robotic NETwork – Ocean Color (AERONET-OC) sampling platform¹², although data from the AERONET-OC are not used in this evaluation. $L_t(748)$ has a value of 0.869713 at this point. We then generated a normally-distributed data set of $L_t(748)$ values with the mean centered at this value and a standard deviation representing a 5% change (i.e., 0.043485 radiance units). From this distribution we drew 50 samples from a total of 21 bins spanning ± 3 standard deviations (thus the bin width is 0.013046).

Thus, by applying noise to $L_t(748)$ we change the value of ϵ . Figure 2 shows the resulting ϵ values for each of the 50 members in the synthetic $L_t(748)$ ensemble data set. Any change in $L_t(748)$ produces a linear change in the calculated ϵ value. As described above, the $L_t(748)$ samples were drawn from a normal distribution, so the ϵ distribution is normal as well (depicted by the red histograms along the X and Y axes in Figure 2).

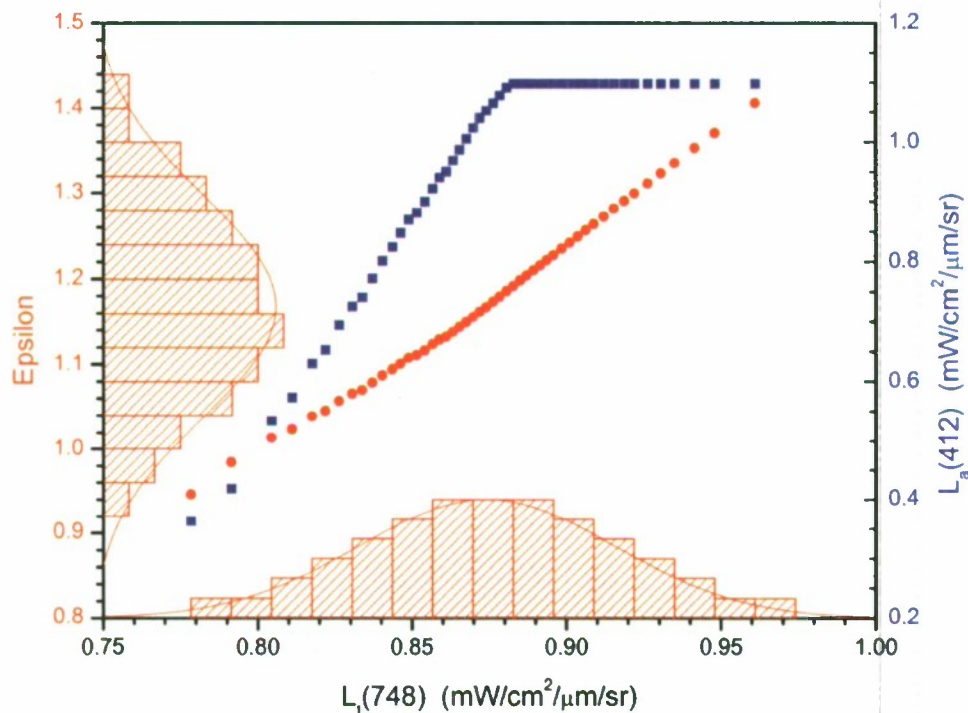


Figure 2. Epsilon vs. $L_t(748)$ [red points, left Y axis], and $L_a(412)$ vs. $L_t(748)$ [blue points, right Y axis] for the test ensemble data set. Histogram along X axis illustrates the normal distribution of the $L_t(748)$ data set; histogram along the left Y axis illustrates the normal distribution of the resulting ϵ data set. The resulting $L_a(412)$ values (blue points) are not normally distributed.

From Figure 2 it is apparent that although a linear change in $L_t(748)$ produces a linear change in ϵ , it does not necessarily produce a linear change in $L_a(412)$. In this test, $L_a(412)$ is linear from approximately 2.2 standard deviations below the mean $L_t(748)$ value, to about 0.2 standard deviations above the mean. Above +0.2 standard deviations, $L_a(412)$ remains constant while ϵ continues to increase. To explain this, we examine the selection of the bounding aerosol models.

In the atmospheric correction scheme, from a suite of 80 aerosol models, two models are selected that bound ϵ ; these two sequential aerosol models are denoted modmin and modmax (modmin is actually the higher number of the two, however). The aerosol model number indicates a specific relative humidity (RH) and aerosol particle size fraction (% fine particle mode); the first numeral in the model number indicates the RH range and the second numeral represents the fine mode fraction. Thus, there are ten size modes for each RH range. For example, model 35 represents a RH in the range 75-80% (indicated by the 3) and a fine mode fraction of 20% (indicated by the 5). The model numbering conventions, RH, and size mode ranges are explained further in a companion paper presented at this conference⁸. Using the near-infrared aerosol radiances ($L_a(748)$, $L_a(869)$), the RH, and the fine mode fraction, spectral $L_a(\lambda)$ at the sensor visible wavelengths are calculated using a radiative transfer model¹³. Then, for a given ϵ obtained for each image pixel, the spectral aerosol radiances at the visible wavelengths are retrieved from a look-up table, by interpolation between the aerosol radiances for the two bounding models selected.

As an example, for a given ϵ , suppose the bounding modmin number selected is 35, then modmax should be 34. However, at the top or bottom of the model number range for a given RH, the modmin and modmax numbers are the same; if a modmin of 30 is selected, then modmax will also equal 30, rather than 29. This is because the aerosol models selected have to stay within the same relative humidity model range (30-39 in this example). The relative humidity is selected before the size fraction, and this prevents the models from escaping the bounds of the current relative humidity range. The same is true at the upper end of the model index range.

Figure 3A shows the bounding aerosol models selected when noise is applied to $L_t(748)$ in this sensitivity test. For our test ensemble data set, at an ϵ value of approximately 1.19 (roughly 0.2 standard deviations above the mean $L_t(748)$ value), modmin and modmax are both 30, meaning that no matter how much more we increase $L_t(748)$, which in turn produces a higher ϵ value, we cannot select new bounding aerosol models. Because the bounding aerosol models are not changing, we continue to retrieve the same look-up value for $L_a(412)$, causing the plateau feature in Figure 2. So, at this location on this day, there is little room for uncertainty, such as calibration errors; variation greater than +0.2 standard deviations for $L_t(748)$ will yield constant $L_a(412)$ retrievals. Thus, in Figure 2, as ϵ increases, $L_a(412)$ increases only to a certain point; once ϵ reaches a certain point, it can no longer be used to compute two new bounding aerosol models. This indicates that perhaps modifications to the model look-up table or radiative transfer model calculations are required to improve the atmospheric correction. We examine the effect of an optimal model selection scheme in a companion paper at this conference⁸.

The $L_a(412)$ value subsequently determines the value of $nL_w(412)$, with higher L_a values leading to lower nL_w values, so the distribution of $nL_w(412)$ in Figure 3B mirrors that of $L_a(412)$ in Figure 2. We then propagated the 50-member ensemble of L_w values through the bio-optical inversion algorithms to estimate chlorophyll (oc3 algorithm¹⁴), $a(412)$, and $b_b(547)$ (QAA algorithm¹⁵). The noise ensemble introduced to the $L_t(748)$ values led to observed differences of -22 to +1%, -75% to +8%, +124% to -10%, for the three bio-optical properties, respectively, from the "original" values (those computed from the image without any noise applied). We are currently extending this single-point $L_t(748)$ ensemble generation approach across an entire ocean color image, to examine spatial variability.

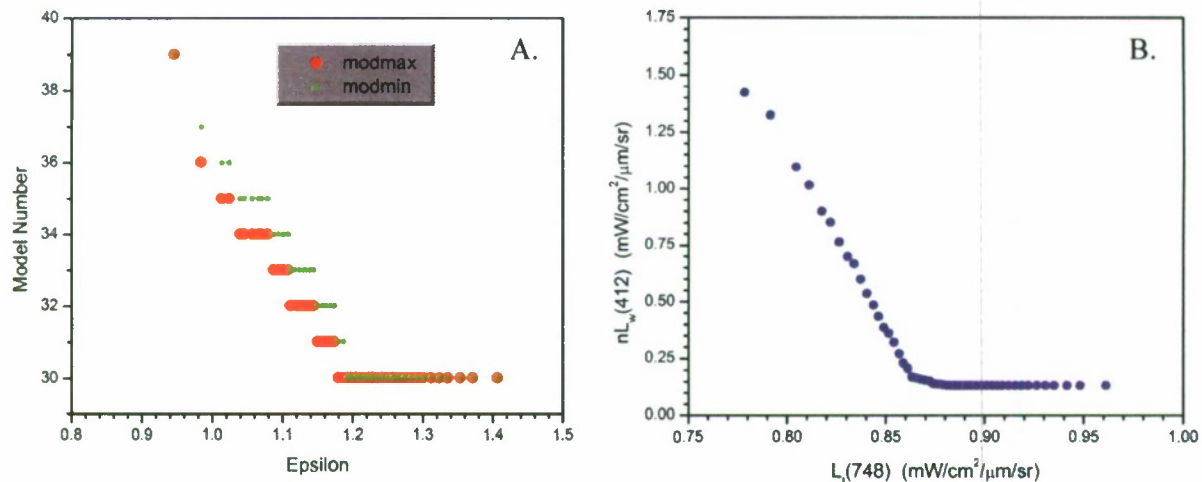


Figure 3. Atmospheric correction results for the test ensemble data set. A. Bounding model number vs. epsilon. B. $nL_w(412)$ vs. $L_t(748)$.

3.2 Simulated sensor degradation

Ocean color sensors in space can degrade over time, due to their exposure to harsh conditions. This leads to erroneous radiance measurements if left uncorrected. For example, over 13 years, the normalized radiances in the 765 nm SeaWiFS band showed a consistent, but non-linear decrease of about 10%, and the 865 nm band decreased by over 20%¹⁶. Temporal calibration changes have been tracked for both the Aqua and Terra MODIS sensors as well^{17,18}. Although the two near-infrared bands are used for atmospheric correction, it is also essential to track the changes in all the bands and apply vicarious corrections². A systematic increase or decrease in the TOA radiance values recorded due to sensor drift or degradation will lead to erroneous estimates of water bio-optical properties. Climate-quality data records (long term, consistent measurements) are required for sensor inter-comparisons and to assess environmental trends, to ensure that any observed data trend is real, and not due to sensor measurement error. For example, accurate, long-term data records are required to determine whether global warming is leading to any concomitant change in global chlorophyll concentrations.

To simulate the effect of sensor drift over time, we applied directional noise to the $L_r(765)$ values for an example SeaWiFS image. Figure 4 shows a SeaWiFS chlorophyll image of the northern Gulf of Mexico collected 26 April 2010. Figure 4A shows the “original” chlorophyll image with no noise applied, and Figure 4B shows the result after applying a 10.5% decrease in $L_r(765)$ at each pixel. Application of the noise led to a decrease in the coastal chlorophyll values and an increase in the offshore chlorophyll values. Keep in mind that the chlorophyll algorithm is multi-banded, so it is influenced by the spectral shape of the water-leaving radiances. Also, the atmospheric correction relies on the two near-infra-red bands, and we are only changing one of those bands. Therefore, there is not a simple relationship between noise applied to one atmospheric correction band and the resulting chlorophyll value.

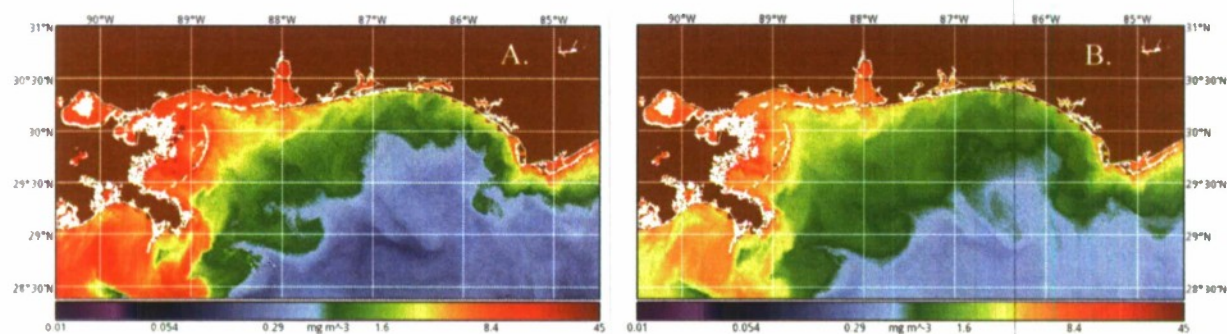


Figure 4. SeaWiFS chlorophyll image covering the northern Gulf of Mexico, 26 April 2010. A. Standard product with no noise applied. B. Result after applying 10.5% decrease in $L_r(765)$ at each image pixel.

3.3 Chlorophyll advection ensembles

The chlorophyll forecast simulations were performed using 16-member ensembles generated from the RELO-NCOM; each ensemble uses a different forcing and initial condition (assumed to be the major sources of error). The perturbations on the initial conditions are set using a technique called Ensemble Transform that re-sets at each re-initialization the variances of the perturbations to match our best guess of the analysis error variances as taken from the Navy Coupled Ocean Data Assimilation (NCODA) system, after assimilation of observations. The atmospheric forcing perturbations are taken from an ensemble population that uses a space-time deformation of the deterministic Coastal Ocean/Atmosphere Mesoscale Prediction System (COAMPS) runs. Essentially this assumes COAMPS has the skill to represent the major surface forcing features, but with slight distortions or/and delays.

The errors in the variable forecasts are determined by multiple sources of uncertainty associated with the model initialization and boundary conditions, numerical approximations, modeling strategies, impact of under-sampling in the assimilation process and unresolved scales. To address the initialization error the best available estimate of analysis error variance as delivered by the data assimilation system is used to transform forecast perturbations into analysis perturbations by finding distinct linear combinations of forecast perturbations. The analysis perturbations are then added to the best available analysis (named control run) to create K initial states. These K initial states are then integrated forward in time using the non-linear model to create the next ensemble forecast. This will be then the starting point for the next transformation that will generate the initial conditions for the subsequent ensemble forecast once the next analysis is available. This technique does not account for additional error sources that could develop during the forecast period through the boundaries and/or through unrepresented numerical errors and approximations.

However, the NCOM ensembles also represent the errors due to uncertain atmospheric forcing by using an ensemble of atmospheric perturbations and allow each ocean run to have an independent atmospheric forcing, therefore augmenting the domain spanned by the ensemble of initial states. For this particular experiment the atmospheric ensemble was generated by atmospheric perturbations using spatially-varying time shifts of the forecast, with a choice of parameters to provide a well developed spread of atmospheric perturbations. This method is mostly adequate when predicted atmospheric fields contain the forecast features of interest, but they are misplaced in space and time.

These ensembles resulting from combining perturbed initialization and atmospheric forcing are used to predict how uncertainties of the ocean fields will evolve in space and time. Typical implementations of ensemble runs use order 40

independent members but this particular experiment only had 16 runs. The ensembles thus represent a suite of model current vectors with varying initial and forcing conditions that simulates uncertainty in the model forecasts. The 16 model current ensembles are then used to create 24, 48, and 72 hour forecasts of the surface chlorophyll distribution by advecting the satellite chlorophyll image. Thus, 16 chlorophyll forecasts are generated from the 16 model ensemble runs, along with a control run (no perturbation of the model initial forcing conditions).

Figure 5 shows the results for the 48 hour forecast (24 and 72-hour results not shown). A cloud-free SeaWiFS image collected on 26 April 2010 covering the Mississippi Bight in the northern Gulf of Mexico was selected for the test (Fig. 5A). The forecast from the control run (Fig. 5B) shows distinct chlorophyll features (due to the fact that we are not presently accounting for diffusion terms in the model); these features are less distinct (more “blurred” or smoothed) in the forecast ensemble mean (Fig. 5C). The normalized standard deviation of the chlorophyll forecast (standard deviation of the 16 ensemble chlorophyll values at each pixel divided by the ensemble mean) is shown in Figure 5D. Only large-scale, offshore currents are constrained in the model ensembles (through assimilation of satellite SSH into RELO-NCOM); coastal currents are not constrained (i.e., no CODAR currents assimilated). This contributes to the high variability in the chlorophyll forecasts observed in the frontal zone area west of the Mississippi River delta, indicating the region where the model currents exhibit the largest variations. Without constraining model current velocities, the uncertainty in the model predictions of the chlorophyll tracer is correspondingly high.

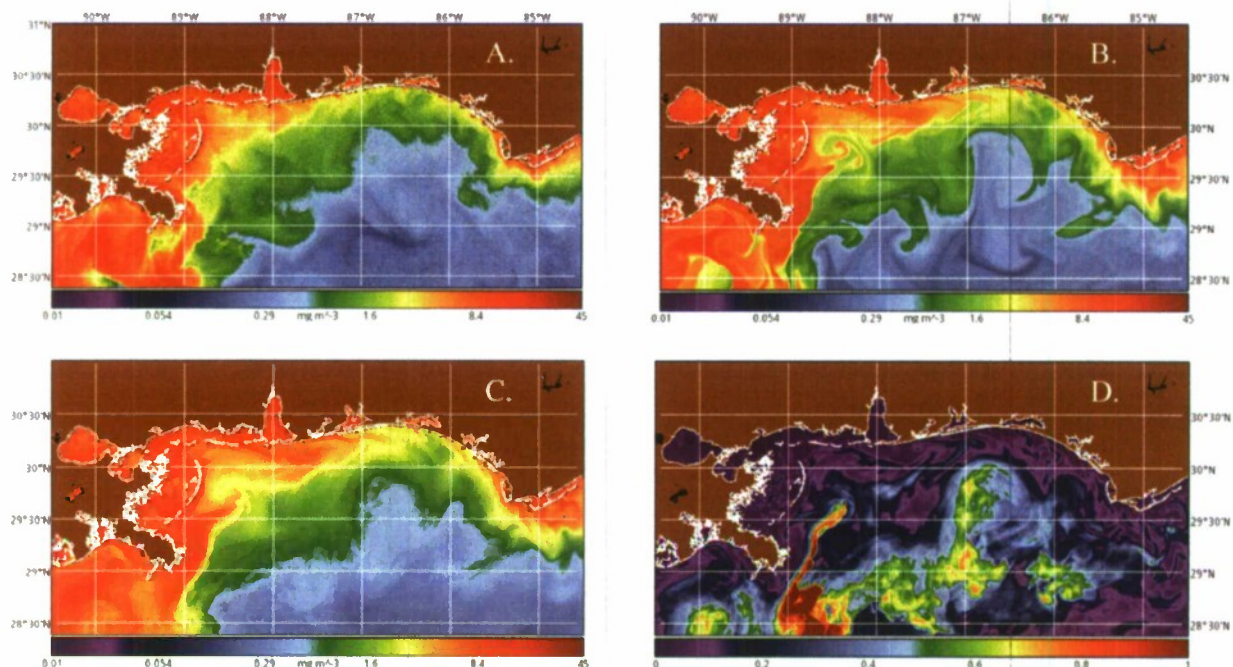


Figure 5. 48-hour chlorophyll forecast simulation, northern Gulf of Mexico. A. Initial SeaWiFS scene from 26 April 2010. B. RELO-NCOM forecast for the control run (no perturbation of initial conditions). C. Mean forecast from the 16-member ensemble runs. D. Normalized standard deviation of the ensemble forecasts.

4. CONCLUSIONS

We have outlined an approach to apply ensemble techniques to estimate uncertainties in satellite-derived bio-optical properties. We addressed uncertainties in the TOA radiances recorded at the sensor, and their propagation to the final bio-optical product estimates. Based on a limited set of single-point error characteristics, initial results indicate that introduction of noise to the TOA radiances at the level of approximately -10% to +10% leads to corresponding errors of -75% to +8% in the derived $a(412)$ values, +124% to -10% in the derived $b_b(547)$ values, and -22 to +1% in the derived chlorophyll values. Initial work to extend this single-point ensemble generation approach spatially across an ocean color

image is underway. We advected a satellite chlorophyll field using a suite of 16 current ensembles derived from a circulation model, and produced mean and standard deviation fields corresponding to a 24, 48, and 72-hour forecasts. These results demonstrate the utility of ensemble techniques to estimate uncertainties of bio-optical properties derived from satellite ocean color imagery.

5. FUTURE WORK

We will continue to employ ensemble techniques to address uncertainties and their propagation at each stage along the satellite ocean color processing path. We will continue to apply and evaluate the single-point ensemble development approach spatially across an entire image, to obtain spatial uncertainty maps for the derived bio-optical properties. In addition, we will examine natural bio-optical variability, using in situ measurements and archived ocean color imagery, to ensure that the ensembles we develop represent reality. We will compare the ensemble probability distribution functions (pdfs) to those from the measured in situ values and adjust the ensembles through application of ensemble transform techniques, and we will apply metrics to evaluate ensemble skill. We will begin to explore the effect of the bio-optical algorithm selection on the satellite bio-optical products, and we will apply ensemble techniques to optimize the bio-optical inversion algorithm coefficients. For example, several of the bio-optical algorithms include coefficients that are applied globally but were estimated empirically using limited data sets (for example, the slope of CDOM spectral absorption and the spectral backscattering coefficient). These coefficients can be adjusted on a regional basis using local in situ training data sets in ensembles. Finally, we will employ super-ensemble techniques to "blend" several bio-optical algorithms to achieve optimal regional performance (lower errors). For example, there are multiple algorithms available for bio-optical inversion, including the QAA, GSM1, PML, and others, and we will examine these algorithms to assess performance in different water types (open-ocean, coastal, turbid). For the bio-optical forecasts, we will attempt to assimilate additional chlorophyll imagery (e.g., satellite imagery from the days following the initial image), and we will assess forecast skill. Finally, we will produce uncertainty maps for the satellite-derived bio-optical properties and their short-term forecasts, by combining the errors propagated along the entire processing path.

ACKNOWLEDGEMENTS

We thank Sherwin Ladner and Brandon Casey for programming assistance. Funding for this work was provided by the Naval Research Laboratory (NRL) internal project "Developing Ensemble Methods to Estimate Uncertainties in Remotely-Sensed Optical Properties (DEMEN)", Program Element 0602435N.

REFERENCES

- [1] Annan, J. D., Hargreaves, J. C., Edwards, N. R., and Marsh, R., "Parameter estimation in an intermediate complexity earth system model using an ensemble Kalman filter," *Ocean Modelling* 8, 135-154 (2005).
- [2] Antoine, D., d'Ortenzio, F., Hooker, S. B., Bécu, G., Gentili, B., Tailliez, D., and Scott, A. J., "Assessment of uncertainty in the ocean reflectance determined by three satellite ocean color sensors (MERIS, SeaWiFS and MODIS-A) at an offshore site in the Mediterranean Sea (BOUSSOLE project)," *J. Geophys. Res.* 113, C07013, doi:10.1029/2007JC004472 (2008).
- [3] Judd, K., Smith, L. A., and Weisheimer, A., "How good is an ensemble at capturing truth? Using bounding boxes for forecast evaluation," *Q. J. R. Meteorol. Soc.* 133, 1309-1325 (2007).
- [4] Rixen, M., and Ferreira-Coelho, E., "Operational surface drift prediction using linear and non-linear hyper-ensemble statistics on atmospheric and ocean models," *J. Mar. Sys.*, doi:10.1016/j.marsys.2004.12.005 (2006).
- [5] Rixen, M., and Ferreira-Coelho, E., "Operational prediction of acoustic properties in the ocean using multi-model statistics," *Ocean Modelling*, doi:10.1016/j.ocemod.2005.02.002 (2005).
- [6] Doblas-Reyes, F. J., Hagedorn, R., and Palmer, T. N., "The rationale behind the success of multi-model ensembles in seasonal forecasting - II. Calibration and combination," *Tellus* 57A, 234-252 (2005).
- [7] Krishnamurti, T. N., Surendran, S., Shin, D. W., Correa-Torres, R. J., Kumar, T. S. V. V., Williford, E., Kummerow, C., Adler, R. F., Simpson, J., Kakar, R., Olson, W. S., and Turk, F. J., "Real-time multianalysis-multimodel superensemble forecasts of precipitation using TRMM and SSM/I products," *Monthly Weather Review* 129, 2861-2883 (2001).

- [8] McCarthy, S. C., Gould, Jr., R. W., Richman, J., Kearney, C., and Lawson, A., "Estimating errors in satellite retrievals of bio-optical properties due to incorrect aerosol model selection," *Proc. SPIE Remote Sensing* (2011).
- [9] Martinolich, P. and Scardino, T., "Automated Processing System User's Guide Version 4.2," NRL, Washington, D.C., http://www7333.nrlssc.navy.mil/docs/aps_v4.2/html/user/aps_chunk/index.xhtml (2011).
- [10] Ko, D. S., Martin, P. J., Rowley, C. D., and Preller, R. H., "A real-time coastal ocean prediction experiment for MREA04," *J. Mar. Syst.* 69, 17-28, doi:10.1016/j.jmarsys.2007.02.022 (2008).
- [11] Gould, Jr., R. W., Green, R. E., Townsend, T. L., Ko, D. S., Flynn, P. M., Blain, C. A., Casey, B., and Arnone, R. A., "Combining Satellite Ocean Color Imagery and Circulation Modeling to Forecast Bio-Optical Properties: Comparison of Models and Advection Schemes," *Proceedings, Ocean Optics XIX Meeting, Italy*, 14pp (2008).
- [12] http://aeronet.gsfc.nasa.gov/new_web/photo_db/Venise.html
- [13] Ahmad, Z., Franz, B. A., McClain, C. R., Kwiatkowska, E. J., Werdell, J., Shettle, E. P., and Holben, B. N., "New aerosol models for the retrieval of aerosol optical thickness and normalized water-leaving radiances from the SeaWiFS and MODIS sensors over coastal regions and open oceans," *Appl. Opt.* 49(29), 5545-5560 (2010).
- [14] O'Reilly, J. E., and 24 Coauthors, "SeaWiFS Postlaunch Calibration and Validation Analyses, Part 3," *NASA Tech. Memo.* 2000-206892, Vol. 11, S.B. Hooker and E.R. Firestone, Eds., NASA Goddard Space Flight Center, 49 pp. (2000).
- [15] Lee, Z., Carder, K.L., and Arnone, R.A., "Deriving inherent optical properties from water color: a multiband quasi-analytical algorithm for optically deep waters," *Appl. Opt.* 41(27), 5755-5772 (2002).
- [16] http://oceancolor.gsfc.nasa.gov/SeaWiFS/On_Orbit/lcal/
- [17] Sun, J., Eplee, R. E., Xiong, X., Stone, T., Meister, G., and McClain, C. R., "MODIS and SeaWiFS On-Orbit Lunar Calibration," *Proc. SPIE* 7081, 70810Y, doi: 10.1117/12.795338 (2008).
- [18] Franz, B. A., Kwiatkowska, E. J., Meister, G., and McClain, C. R., "Moderate Resolution Imaging Spectroradiometer on Terra: limitations for ocean color applications," *J. Appl. Rem. Sens.* 2, 023525, doi: 10.1117/1.2957964 (2008).